Published in final edited form as:
Arterioscler Thromb Vasc Biol. 2010 January ; 30(1): 54. doi:10.1161/ATVBAHA.109.196386.

MOLECULAR IMAGING OF THE INITIAL INFLAMMATORY RESPONSE IN ATHEROSCLEROSIS: IMPLICATIONS FOR EARLY DETECTION OF DISEASE

Beat A. Kaufmann, MD, **Chad L. Carr, MD**, **J. Todd Belcik, BS RDCS**, **Aris Xie, BS**, **Qi Yue, MD**, **Scott Chadderdon, MD**, **Evan S. Caplan**, **Jaspreet Khangura, MD**, **Sherry Bullens, BA**, **Stuart Bunting, PhD**, and **Jonathan R. Lindner, MD**
Division of Cardiovascular Medicine, Oregon Health & Science University Portland, OR (BAK, CLC, JTB, AX, QY, SC, ESC, JK, JRL); and the Department of Tumor Biology and Angiogenesis, Genentech Inc., South San Francisco, CA (SB, SB)

Abstract

Background—We hypothesized that molecular imaging of endothelial cell adhesion molecule expression could non-invasively evaluate pre-lesion pro-atherogenic phenotype.

Methods—Mice deficient for the LDL-receptor and the Apobec-1 editing peptide (DKO mice) were studied as an age-dependent model of atherosclerosis. At 10, 20, and 40 weeks of age, ultrasound molecular imaging of the proximal thoracic aorta was performed with contrast agents targeted to P-selectin and VCAM-1. Atherosclerotic lesion severity and content were assessed by ultra-high frequency ultrasound, histology, and immunohistochemistry.

Results—In wild-type mice at all ages, there was neither aortic thickening nor targeted tracer signal enhancement. In DKO mice, lesions progressed from sparse mild intimal thickening at 10 weeks to widespread severe lesions with luminal encroachment at 40 weeks. Molecular imaging for P-selectin and VCAM-1 demonstrated selective signal enhancement ($p<0.01$ vs. non-targeted agent) at all ages for DKO mice. P-selectin and VCAM-1 signal in DKO mice were greater by 3-fold at 10 wks, 4–6-fold at 20 wks, and 9–10-fold at 40 weeks compared to wild-type mice. En face microscopy demonstrated preferential attachment of targeted microbubbles to regions of lesion formation.

Conclusions—Non-invasive ultrasound molecular imaging of endothelial activation can detect lesion-prone vascular phenotype before the appearance of obstructive atherosclerotic lesions.

The inflammatory response plays an important role in the initiation and progression of atherosclerosis and the susceptibility to acute ischemic syndromes. Novel methods for detecting vascular inflammation are being developed in order to better ascertain risk for adverse events. One strategy is to directly visualize the molecular or cellular components of the immune response with targeted imaging probes. This approach could also potentially be used for early identification of individuals predisposed to severe atherosclerosis by detecting phenotypic changes that occur decades before clinical manifestations arise.[1]

The aim of this study was to test whether the early and inciting events of atherosclerosis can be detected *in vivo* by molecular imaging. The targets for this study, VCAM-1 and P-selectin, are key endothelial cell adhesion molecules that regulate leukocyte trafficking in

Address correspondence to: Jonathan R. Lindner, MD Cardiovascular Division, UHN-62 Oregon Health & Science University 3181 SW Sam Jackson Park Rd. Portland, OR 97239 Tel. (503) 494-8750 Fax (503) 494-8550 lindnerj@ohsu.edu.

DISCLOSURES Dr. Lindner serves on the Scientific Advisory Board for VisualSonics Inc.

atherosclerosis.[2–5] Surface expression of both of these molecules occurs in response to oxidized LDL cholesterol and are present early at lesion-prone sites.[2–10] Most targeted imaging technologies have been tested in models where plaque formation and inflammatory cell influx are advanced. However, *ex-vivo* microscopy studies have demonstrated that imaging probes targeted to VCAM-1 and/or P-selectin accumulate in early atherosclerotic lesions.[11,12] In this study, we hypothesized that molecular imaging *in vivo* could detect upregulation of adhesion molecules before the development of advanced atherosclerotic lesions. To test our hypothesis, targeted imaging and histomorphometric analysis were performed at various ages in mice with a genetic deletion of both the LDL receptor and the apolipoprotein (Apo) mRNA editing protein Apobec-1 that is responsible for preferential transcription of ApoB-48 over ApoB-100 in mice.[13,14] These double knockout (DKO) mice have high circulating LDL cholesterol with full length ApoB-100 and develop a predictable age-dependent course of atherosclerosis in the proximal aorta and all branch points while on a chow diet.[14]

METHODS

Study Design

The study was approved by the Animal Care and Use Committee of the Oregon Health & Science University. Control wild-type C57Bl/6 mice and 33 DKO mice with gene-targeted deletion of the LDL receptor and Apobec-1 on a C57Bl/6 background underwent imaging studies at 10, 20 or 40 weeks of age (n=7 to 10 for each strain at each age). Approximately half of the mice were euthanized after either the 10 or 20 wks imaging study for aortic histomorphometry and immunohistochemistry for adhesion molecule expression. Total lesion area from *en face* Oil Red O staining of aortic whole mounts was performed in an additional 15 DKO mice (n=5 for each age). Spatial characterization of adhesion for fluorescently-labeled targeted microbubbles was assessed from *ex vivo* microscopy of the aortic arch in DKO mice.

Microbubble Preparation

Biotinylated lipid-shelled decafluorobutane microbubbles were prepared by sonication of a g a s-saturated aqueous suspension of distearoylphosphatidylcholine and distearoylphosphatidylethanolamine-PEG(2000)biotin (Avanti Polar Lipids, Alabaster AL). Rat anti-mouse monoclonal IgG_1 against either VCAM-1 (MK 2.7) or P-selectin (RB40.34), or isotype control antibody (R3-34, Pharmingen Inc.) were conjugated to the surface of microbubbles as previously described to produce control, P-selectin-targeted or VCAM-1-targeted microbubbles.[15,16] The control preparation has been shown to result in minimal non-specific attachment *in vivo* and in flow chamber models with cultured endothelial cells.[15,16] Microbubble size distribution and concentration were measured by electrozone sensing (Multisizer III, Beckman Coulter, Fullerton, CA). Size distribution was not different between agents nor was the surface density of ligand determined by flow cytometry (saturating concentration at 20 μg per 1×10^8 microbubbles for all three agents).[15]

Targeted Imaging of VCAM-1 and P-selectin

Mice were anesthetized with inhaled isoflurane. A jugular vein was cannulated using sterile technique. Contrast-enhanced ultrasound (CEU) of the aorta was performed with a high-frequency linear-array probe (Sequoia, Siemens Medical Systems, Mountain View, CA) fixed in place by railed gantry system. The ascending aorta, proximal aortic arch, and proximal brachiocephalic trunk were imaged in long axis using a right parasternal imaging approach. For CEU, the non-linear fundamental signal component for microbubbles was detected with a multipulse protocol (Contrast Pulse Sequencing™) at a transmission frequency of 7 MHz, a mechanical index of 1.1–1.2, and a dynamic range of 40 dB. Gain settings were adjusted to levels just below visible noise speckle and held constant. These settings provide a linear and reproducible relationship between contrast concentration and intensity obtained in the study

(see online supplement Figure A). Images were acquired 10 minutes after the intravenous injection of targeted or control microbubble agents (1×10^6 per injection, performed in random order). After several frames were acquired at a pulsing interval (PI) of 1s, the mechanic index was briefly increased to 1.5–1.7 to completely null microbubble signal then several frames were acquired at a PI of 5 s to measure the signal from freely circulating microbubbles. Video intensities were transformed from a log-compressed to linear scale using the log function for the ultrasound system. Several post-destruction frames were averaged and digitally subtracted from the first two predestruction frames to derive signal from retained microbubbles only (see online supplement Figure B).[15] Intensity was measured from a region-of-interest placed around the ascending aorta and aortic arch and extending into the origin of the brachiocephalic artery. Region selection was guided by fundamental frequency imaging at 14 MHz acquired at the end of each CEU acquisition. *In vitro* water bath experiments were performed with the *in vivo* settings using incremental microbubble concentrations in a 2 L water bath with a stir bar. A total of 5 frames at a PI of 1 s were analyzed and averaged.

Plaque Morphometry by Ultrasound

High-resolution imaging of the aortic arch was performed with a high-frequency (40MHz) imaging system with an integrated physiology monitoring platform (Vevo 770, VisualSonics Inc., Toronto, Canada). Measurements were made at end-diastole by gating individual line acquisition to the electrocardiogram (frame rate of ≈1,000 Hz). Plaque burden was assessed by measuring vessel wall thickness at the lesser curvature of the arch and the origin of the brachiocephalic artery (intraobserver variability 7±3%, interobserver variability <15%). Left ventricular fractional shortening, averaged for the two short-axis diameters, was assessed in the parasternal short axis plane at the mid-papillary muscle level. Centerline peak systolic velocity was measured with pulsed-wave Doppler with the sample volume placed in the aortic arch just distal to the brachiocephalic artery.

Ex vivo Imaging of Microbubble Adhesion

In anesthetized DKO mice at 20 or 40 weeks of age (n=3 for each), P-selectin- or VCAM-1-targeted microbubbles (1×10^6) fluorescently labeled with the dialkylcarbocyanine fluorochrome DiI were injected via a jugular vein. Control microbubbles (1×10^6) labeled with DiO were injected simultaneously. After 3 min of circulation time, the blood volume of the mouse was removed by infusion of 8 mL isothermic heparinized saline at physiologic pressure through a left ventricular puncture. The thoracic aorta was removed, incised longitudinally, and pinned to allow *en face* observation of the endothelial surface. Microbubble attachment relative to plaque development was characterized using fluorescent epi-illumination (excitation filter 460–490 nm and 530–560 nm).

Histology

For histology, perfusion fixation was performed and short axis sections of the mid ascending aorta and proximal arch just prior to the brachiocephalic artery were snap-frozen providing two separate regions for each subject. Movat's pentachrome stain was performed for assessment of plaque area measured by the tissue area within the internal elastic lamina. For immunohistology of VCAM-1 expression, a goat polyclonal antibody for VCAM-1 (sc1504, Santa Cruz Biotechnology Inc.) with secondary peroxidase staining (ABC Vectastain Elite, Vector Laboratories) was used. Since P-selectin is pre-stored within endothelial cells, surface expression was evaluated by *in vivo* labeling. Streptavidin Qdot nanocrystals (Invitrogen, 605 nm peak emission spectrum) bearing Rb40.34 were injected intravenously (20 μL) in 2 wild-type and 4 DKO mice at 10 or 40 wks of age. The blood volume was rinsed by ventricular infusion and the aorta was dissected free, incised longitudinally, and observed under fluorescent illumination. Determination of *en face* plaque area for the thoracic aorta was

determined from methanol-fixed (78%) whole mounts stained with 0.15% Oil Red O (Sigma Aldrich).

Statistical Analysis

Data were analyzed on SAS (version 9.1) or RS/1 (version 6.0.1, Domain Manufacturing Corp). Data were analyzed with one-way ANOVA for normally distributed variables with post-hoc testing of individual comparisons with paired t-test, or by the Wilcoxon rank-sum test for medians. Bonferroni correction was applied for multiple comparisons. A Spearman rank correlation test was used to assess the relationship between age and histology data.

RESULTS

Cardiac Performance and Aortic Flow Velocities

On echocardiography left ventricular fractional shortening, aortic internal diameter, and aortic peak systolic flow velocities were similar for DKO and wild-type mice at each age (Table 1). These data indicate that hemodynamic and shear rates that can influence microbubble adhesion in the aorta were similar between groups.

Vessel Morphometry and Histology

Oil Red O staining of aortic whole mounts detected an age-dependent increase in plaque *en face* area in DKO mice whereas staining was essentially absent in wild-type animals (Figure 1A). On histology with Movat's staining (Figure 1B), there was no intimal thickening in wild-type mice at any age. In DKO mice, at 10 weeks of age there were regions of mild intimal thickening and occasional monocyte adhesion to the endothelial surface seen in several animals, although the majority of sections had no significant abnormalities. At 20 weeks of age, small but discrete fibrous or fibrofatty lesions were frequently detected and were often associated with disruption of the elastic lamina. These lesions rarely encroached into the lumen area. All sections from 40 week-old DKO mice demonstrated severe lipid-rich lesions with abundant inflammatory cells and regions of necrosis. These lesions tended to protrude well into the aortic lumen.

Vessel wall thickness measured by ultra-high frequency ultrasound of was ≤60 μm in wild-type mice and did not change with age (Figure 2, Supplemental Video 1). In DKO mice, wall thickness at 10 weeks of age was similar to wild-type mice. At 20 weeks, there was a small increase in arterial wall thickness in DKO mice that did not reach statistical significance, indicating that the small lesions seen on histology could not be reliably detected by high-frequency ultrasound. At 40 wks of age, ultrasound detected marked arterial thickening \of the lesser curvature of the aorta and focal plaque formation at the proximal brachiocephalic artery (Figure 2, Supplemental Video 2).

On immunohistochemistry for VCAM-1, there was minimal staining in wild-type mice at all ages. In DKO mice, VCAM-1 was present on the intimal surface at 10, 20, and 40 weeks of age (Figure 3A–3D). At 40 weeks of age, VCAM-1 was particularly intense on the endothelium at shoulder regions and within the complex lesions containing immune cells. Aortic whole mounts with *in vivo* labeling with P-selectin-targeted Q-dots demonstrated endothelial surface expression of P-selectin only in DKO mice, particularly at sites of lesion formation (on-line supplemental data).

Targeted Imaging of Adhesion Molecule Expression

Fluorescent microscopy of aortic whole mounts revealed attachment of both P-selectin and VCAM-1-targeted microbubbles diffusely on the surface of regions of early plaque formation in 20 wk DKO mice (Figure 3E and 3F, additional images available in the on-line supplemental

data). Adhesion was particularly dense along the proximal margins of the plaques. Adhesion to normal regions was sparse except at the origin of intercostal branches in the descending portion of the thoracic aorta. In 40 wk DKO mice, targeted microbubble adhesion was again more frequent in regions of plaque formation, although preferential adhesion at the plaque margins was much less prominent than at 20 wks. Irrespective of age, targeted microbubble adhesion was most dense in lesions at the origin of the brachiocephalic artery. Control microbubble attachment was rare and not related to any particular plaque topography.

CEU molecular imaging signal in the ascending aorta and arch of wild-type mice was similar between control microbubbles and targeted microbubbles (Figure 4A). In DKO mice there was selective signal enhancement for P-selectin and VCAM-1-targeted microbubbles compared to control microbubbles at 10, 20, and 40 wks of age. Signal from stationary targeted microbubbles occurred at both the specular edges of the vessel and "within the lumen" due to volume averaging of the entire mouse aorta within the elevational profile of the beam.[16] P-selectin and VCAM-1 signal in DKO mice was greater than wild type controls at all time points. The ratio of targeted signal in DKO mice versus control mice increased with age (approximately 3-fold greater at 10 wks, 4–6-fold greater at 20 wks, and 9–10-fold at 40 wks). A diffuse pattern of enhancement throughout the aortic arch was seen in 40 wk DKO mice (illustrated in Figure 4). Signal enhancement at the early time intervals (10 and 20 weeks) was often focal, illustrated in Figure 5 which also demonstrates how spatial localization was performed. A linear relation between the microbubble concentration and CEU intensity was found from *in vitro* water bath experiments (Figure 6).

DISCUSSION

Up-regulation and surface expression of vascular endothelial cell adhesion molecules are early events in atherogenesis. Results from this study performed in a reproducible age-dependent murine model of aortic atherosclerosis indicate that molecular imaging of pathogenic endothelial cell adhesion molecules such as VCAM-1 and p-selectin can detect atheresclerotic vascular phenotype before the development of advanced lesions.

Over the past decade, there has been increasing interest in the development of molecular imaging methods to assess the inflammatory response in atherosclerotic disease. Probe design has been governed by the intended clinical use. For example, the differentiation of high-risk "vulnerable" disease from more stable disease requires a technique that can detect the tempestuous late-stage events that contribute to plaque rupture or erosion. These events include macrophage infiltration, endothelial cell activation, protease activity, chemokine production, thinned fibrous cap, and increased metabolic activity. The aim of this study was to determine whether a molecular imaging approach could unmask early pathophysiologic changes and reveal risk for future development of severe disease. The scope of potential targets that can identify very early atherosclerosis is narrower than those for high-risk late-stage disease. One strategy has been to image the accumulation of oxidized lipoproteins in the vessel wall.[17,18] In this study, our approach was to image the secondary inflammatory responses that occur in response to oxidized lipids by targeting microbubbles to adhesion molecules that are preferentially expressed at disease-prone regions.[2–10]

Interactions between P-selectin on the endothelial cell surface and modified glycoprotein counterligands on leukocytes mediates rolling and activation of leukocytes in post-capillary venules.[19,20] These events are requisite for firm arrest and transmigration. Slow rolling and firm adhesion are, in part, mediated by interaction between leukocyte VLA-4 ($\alpha_4\beta_1$) and VCAM-1 on the endothelial surface. The selection of P-selectin and VCAM-1 as endothelial markers of early disease was based not solely on their importance in the inflammatory response.

These molecules play a critical role in leukocyte arrest in high-shear stress vessels such as the mouse aorta,[21] and participate in the early stages of atherogenesis.[4,5]

It has been previously shown that expression of endothelial cell adhesion molecules such as VCAM-1 and P-selectin in *advanced* atherosclerotic disease can be imaged *in vivo* with ultrasound or MRI targeted imaging probes.[11,12,16,22,23] VCAM-1 signal intensity on CEU has been shown to correlate with the severity of diet-modulated vascular inflammation in late stage ApoE−/− mice.[16] Feasibility for detecting disease at an *early* stage has been suggested by *ex vivo* optical imaging of aortas from ApoE−/− mice where accumulation of VCAM-1-targeted optical probes can be observed at the site non-obstructive atherosclerotic lesions.[11, 12]

In the present study we show for the first time that it is possible to non-invasively image vascular inflammation in atherosclerosis at the onset of inflammatory cell entry into the vessel wall before the development of intimal xanthomas (fatty streaks). It was interesting to note that targeted signal enhancement in DKO mice was relatively consistent between ages, which could reflect a constant pattern of endothelial expression, despite and increase in intraplaque VCAM-1 signal exemplified in Figure 3. However, signal enhancement for microbubbles targeted to P-selectin and VCAM-1 in DKO *relative* to wild-type mice did increase with age, possibly reflecting a limitation in using a fixed dose of contrast agent rather than indexed to weight. The age-related increase in *en face* plaque area and cross-sectional plaque area on Movat's staining outpaced the age-related increase in targeted signal for DKO versus wild type animals. Based on the spatial pattern of microbubble attachment, we believe that minimal increase in signal despite increasing plaque area could also reflect the preferential expression of adhesion molecules such as VCAM-1 that occurs at the margins rather than the central "dome" of plaques.[6,7]

We believe that the detection of very early immune responses is an ideal application for molecular imaging with a CEU approach. Since early identification of pro-atherogenic vascular phenotype is likely to be used as a screening tool, the brevity of CEU molecular imaging protocols and availability of ultrasound in the outpatient setting are practical advantages. Transition to humans will be contingent on development of probes suitable for human use in terms of conjugation chemistry and ligand composition such as peptides that have been discovered through phage-display screening.[23]

There are several limitations of this study that deserve attention. We cannot yet draw any conclusions regarding whether disease management can be improved by molecular imaging of the early inflammatory response. Although ultra-high-frequency imaging was able to evaluate focal aortic thickening, the lower-frequency contrast-specific imaging method did not provide adequate spatial resolution to colocalize signal enhancement with degree of thickening. This issue is related to the small scale of the animal model used and the phenomenon of volume averaging that occurs when the full dimension of the mouse aorta fits within the beam elevation.[16] It is likely that high-frequency ultrasound measurements overestimated the relative degree of aortic thickening in 40 week DKO mice compared to controls, largely because the axial resolution (approximately 50–70 μm) precluded true representation of normal wall dimensions. The data do, however, support the notion that molecular imaging can detect the molecular signature of disease before even the most sensitive of techniques for evaluating morphology. We also did not evaluate the relative contribution of platelets to p-selectin signal enhancement,[24] although histology studies did not show evidence of significant platelet thrombi.

In conclusion, we show that CEU molecular imaging can be used to noninvasively detect the expression of cell adhesion molecules that are involved in the early pathogenesis of atherosclerosis. These inflammatory changes can be imaged non-invasively before the

development of advanced lesions. This method could in the future be useful for early risk stratification in atherosclerosis.

Supplementary Material

Refer to Web version on PubMed Central for supplementary material.

Acknowledgments

FUNDING SOURCES These studies were supported by grants R01-HL-074443, R01-HL-078610, and R01-DK-063508 to Dr. Lindner from the National Institutes of Health, and from a grant from Genentech Inc. Dr. Kaufmann is supported by a research grant from the Lichtenstein Foundation. Dr. Carr is supported by a Post-doctoral Fellowship Grant from the Pacific Mountain Affiliate of the American Heart Association. Dr. Chadderdon is supported by a Fellow to Faculty Transition Award from the American Heart Association.

REFERENCES

1. Strong JP, Malcom GT, McMahan CA, Tracy RE, Newman WP, Herderick EE, Cornhill JF. Prevalence and extent of atherosclerosis in adolescents and young adults: implications for prevention from the Pathobiological Determinants of Atherosclerosis in Youth Study. JAMA 1999;281:727–735. [PubMed: 10052443]
2. Cybulsky MI, Iiyama K, Li H, Zhu S, Chen M, Iiyama M, Davis V, Gutierrez-Ramos JC, Connelly PW, Milstone DS. A major role for VCAM-1, but not ICAM-1, in early atherosclerosis. J Clin Invest 2001;107:1255–1262. [PubMed: 11375415]
3. Dansky HM, Barlow CB, Lominska C, Sikes JL, Kao C, Weinsaft J, Cybulsky MI, Smith JD. Adhesion of monocytes to arterial endothelium and initiation of atherosclerosis are critically dependent on vascular cell adhesion molecule-1 gene dosage. Arterioscler Thromb Vasc Biol 2001;21:1662–1667. [PubMed: 11597942]
4. Johnson RC, Chapman SM, Dong ZM, Ordovas JM, Mayadas TN, Herz J, Hynes RO, Schaefer EJ, Wagner DD. Absence of P-selectin delays fatty streak formation in mice. J Clin Invest 1997;99:1037–1043. [PubMed: 9062362]
5. Dong ZM, Chapman SM, Brown AA, Frenette PS, Hynes RO, Wagner DD. The combined role of P- and E-selectins in atherosclerosis. J Clin Invest 1998;102:145–152. [PubMed: 9649568]
6. Iiyama K, Hajra L, Iiyama M, Li H, DiChiara M, Medoff BD, Cybulsky MI. Patterns of vascular cell adhesion molecule-1 and intercellular adhesion molecule-1 expression in rabbit and mouse atherosclerotic lesions and at sites predisposed to lesion formation. Circ Res 1999;85:199–207. [PubMed: 10417402]
7. Nakashima Y, Raines EW, Plump AS, Breslow JL, Ross R. Upregulation of VCAM-1 and ICAM-1 at atherosclerosis-prone sites on the endothelium in the ApoE-deficient mouse. Arterioscler Thromb Vasc Biol 1998;18:842–851. [PubMed: 9598845]
8. Khan BV, Parthasarathy SS, Alexander RW, Medford RM. Modified low density lipoprotein and its constituents augment cytokine-activated vascular cell adhesion molecule-1 gene expression in human vascular endothelial cells. J Clin Invest 1995;95:1262–1270. [PubMed: 7533787]
9. Ramos CL, Huo Y, Jung U, Ghosh S, Manka DR, Sarembock IJ, Ley K. Direct demonstration of P-selectin- and VCAM-1-dependent mononuclear cell rolling in early atherosclerotic lesions of apolipoprotein E-deficient mice. Circ Res 1999;84:1237–1244. [PubMed: 10364560]
10. Mehta A, Yang B, Khan S, Hendricks JB, Stephen C, Mehta JL. Oxidized low-density lipoproteins facilitate leukocyte adhesion to aortic intima without affecting endothelium-dependent relaxation. Role of P-selectin. Arterioscler Thromb Vasc Biol 1995;15:2076–2083. [PubMed: 7583592]
11. Nahrendorf M, Jaffer FA, Kelly KA, Sosnovik DE, Aikawa E, Libby P, Weissleder R. Noninvasive vascular cell adhesion molecule-1 imaging identifies inflammatory activation of cells in atherosclerosis. Circulation 2006;114:1504–1511. [PubMed: 17000904]
12. McAteer MA, Schneider JE, Ali ZA, Warrick N, Bursill CA, von zur Muhlen C, Greaves DR, Neubauer S, Channon KM, Choudhury RP. Magnetic resonance imaging of endothelial adhesion

molecules in mouse atherosclerosis using dual-targeted microparticles of iron oxide. Ateriosclerosis Thromb Vasc Biol 2008;28:77–83.

13. Farese RV, Véniant MM, Cham CM, Flynn LM, Pierotti V, Loring JF, Traber M, Ruland S, Stokowski RS, Huszar D, Young SG. Phenotypic analysis of mice expressing exclusively apolipoprotein B48 or apolipoprotein B100. Proc Natl Acad Sci USA 1996;93:6396–6398.
14. Powell-Braxton L, Veniant M, Latvala RD, Hirano KI, Won WB, Ross J, Dybdal N, Zlot CH, Young SG, Davidson NO. A mouse model of human familial hypercholesterolemia: markedly elevated low density lipoprotein cholesterol levels and severe atherosclerosis on a low-fat chow diet. Nat Med 1998;4:934–938. [PubMed: 9701246]
15. Lindner JR, Song J, Christiansen J, Klibanov AL, Xu F, Ley K. Ultrasound assessment of inflammation and renal tissue injury with microbubbles targeted to P-selectin. Circulation 2001;104:2107–2112. [PubMed: 11673354]
16. Kaufmann BA, Sanders JM, Davis C, Xie A, Aldred P, Sarembock IJ, Lindner JR. Molecular imaging of inflammation in atherosclerosis with targeted ultrasound detection of vascular cell adhesion molecule-1. Circulation 2007;116:276–284. [PubMed: 17592078]
17. Tsimikas S, Palinski W, Halpern SE, Yeung DW, Curtiss LK, Witztum JL. Radiolabeled MDA2, an oxidation-specific, monoclonal antibody, identifies native atherosclerotic lesions in vivo. J Nucl Cardiol 1999;6:41–53. [PubMed: 10070840]
18. Briley-Saebo KC, Shaw PX, Mulder WJ, Choi SH, Vucic E, Aguinaldo JG, Witztum JL, Fuster V, Tsimikas S, Fayad ZA. Targeted molecular probes for imaging atherosclerotic lesions with magnetic resonance using antibodies that recognize oxidation-specific epitopes. Circulation 2008;117:3206–3215. [PubMed: 18541740]
19. Ley K, Bullard DC, Arbones ML, Bosse R, Vestweber D, Tedder TF, Beaudet AL. Sequential contribution of L- and P-selectin to leukocyte rolling in vivo. J Exp Med 1995;181:669–675. [PubMed: 7530761]
20. Chigaev A, Waller A, Zwartz GJ, Buranda T, Sklar LA. Regulation of cell adhesion by affinity and conformational unbending of alpha4beta1 integrin. J Immunol 2007;178:6828–6839. [PubMed: 17513731]
21. Eriksson EE, Werr J, Guo Y, Thoren P, Lindbom L. Direct observations in vivo on the role of endothelial selectins and alpha(4) integrin in cytokine-induced leukocyte-endothelium interactions in the mouse aorta. Circ Res 2000;86:526–533. [PubMed: 10720414]
22. Hamilton AJ, Huang SL, Warnick D, Rabbat M, Kane B, Nagaraj A, Klegerman M, McPherson DD. Intravascular ultrasound molecular imaging of atheroma components in vivo. J Am Coll Cardiol 2004;43:453–460. [PubMed: 15013130]
23. Kelly KA, Allport JR, Tsourkas A, Shinde-Patil VR, Josephson L, Weissleder R. Detection of vascular adhesion molecule-1 expression using a novel multimodal nanoparticle. Circ Res 2005;96:327–336. [PubMed: 15653572]
24. Burger PC, Wagner DD. Platelet P-selectin facilitates atherosclerotic lesion development. Blood 2003;101:2661–2666. [PubMed: 12480714]

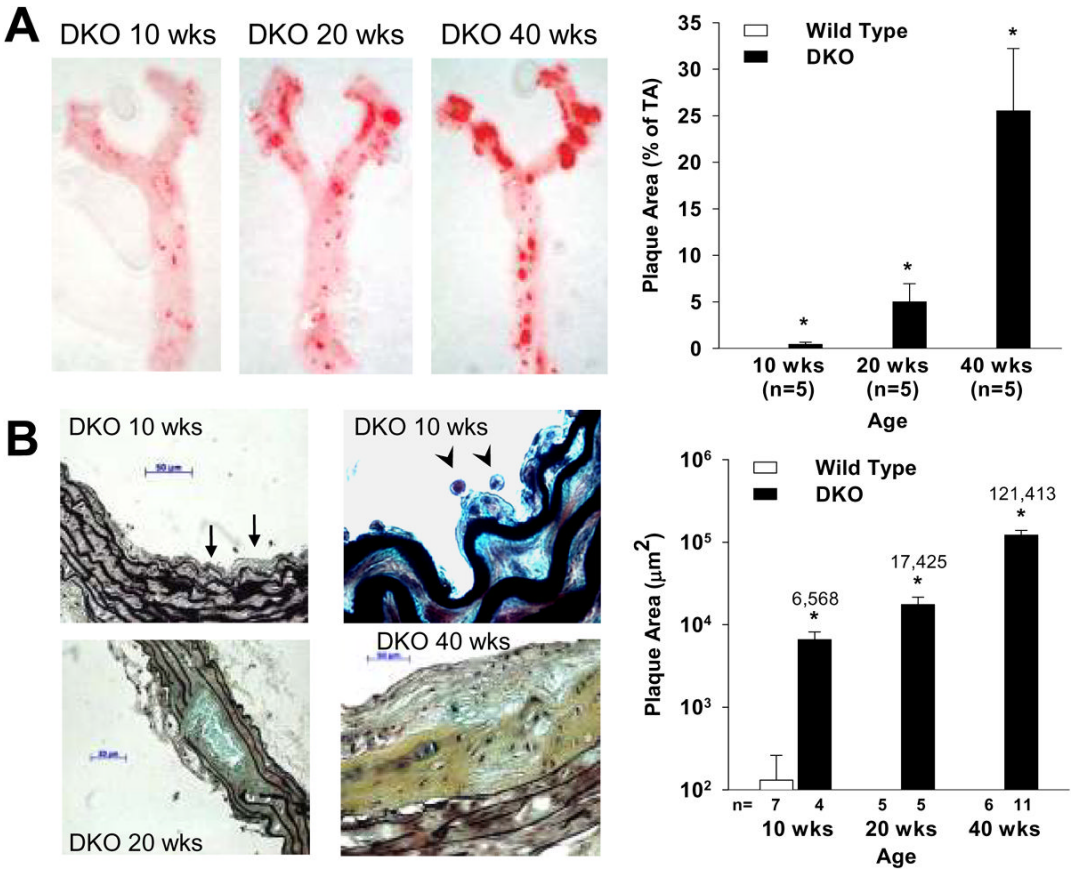

Figure 1.

Representative images and plaque area data on histology. (**A**) Oil Red-O staining of aorta whole mounts show an increase in lesion area with age (Spearman rank correlation coefficient 0.94; $p<0.001$). Mean (±SEM) area data are displayed as percent of the total area of the thoracic aorta (TA). (**B**) Movat's pentachrome stains of the thoracic aorta and mean (±SEM) lesion area from axial sections displayed on a log scale. Images from DKO mice at 10 weeks demonstrate examples of very mild intimal thickening (arrows) and mononuclear cell adhesion to the endothelial surface (arrowheads). Lesion area increased with age for DKO mice (Spearman rank correlation coefficient 0.76; $p<0.001$). *$p<0.01$ vs wild-type.

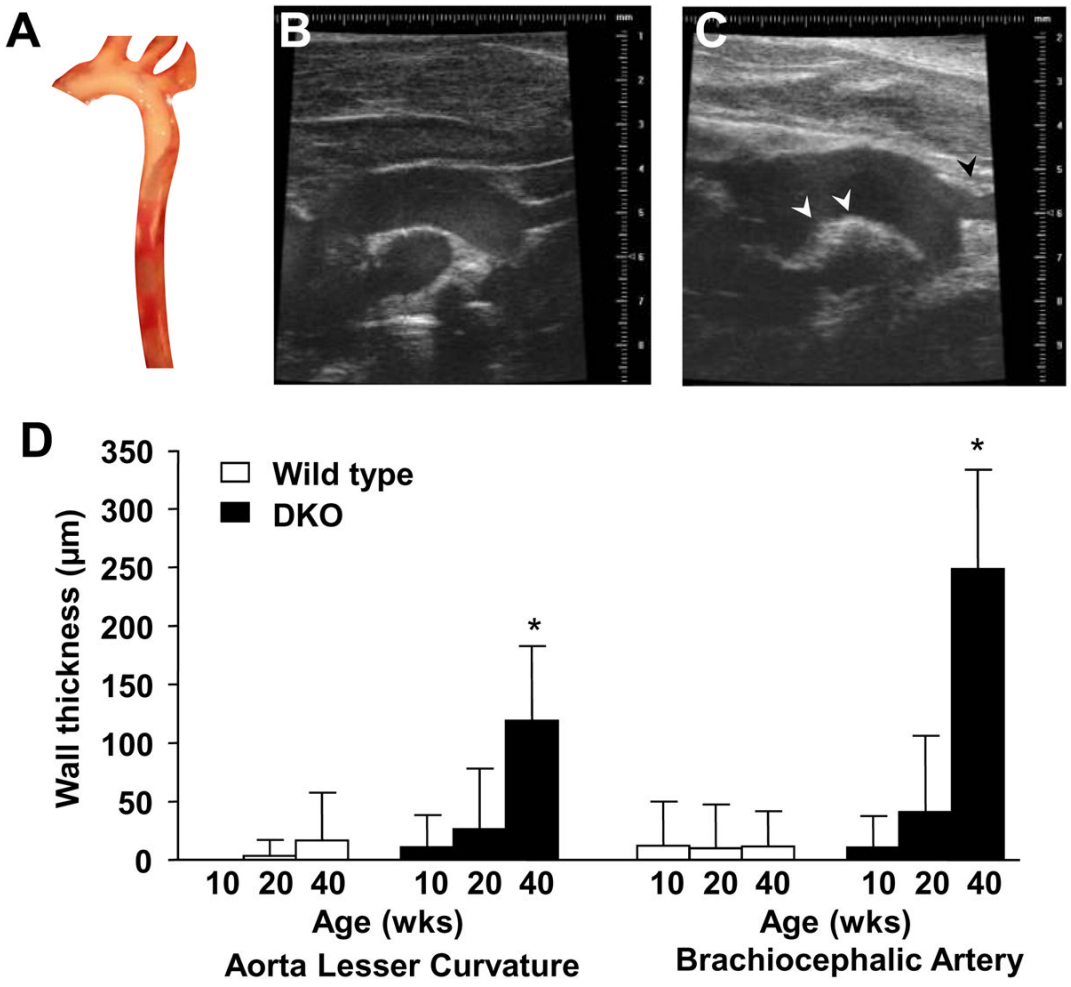

Figure 2.

High frequency ultrasound morphometry of the thoracic aorta. **(A)** Intact aorta from a DKO mouse *in situ* demonstrating severe lipid-rich atherosclerotic lesions in the proximal aorta and arch vessels. Surrounding anatomic structures were masked. Ultrasound images (40 MHz) of the aorta in its long-axis from the aortic valve level to the mid arch from are shown for a wild-type **(B)**, and DKO **(C)** mouse. In the DKO mouse, there is discrete plaque formation in the proximal brachiocephalic artery (black arrow) and severe thickening of the lesser curvature (white arrows) between the aortic lumen and right pulmonary artery. **(D)** Mean (±SEM) vessel wall thickness measured at the lesser curvature of the aorta and the brachiocephlic artery. N=10,10,7 for wild-type mice at 10, 20, 40 wks of age, respectively. N=13, 11, 12 for DKO mice at 10, 20, 40 wks of age, respectively. *$p<0.01$ vs wild type.

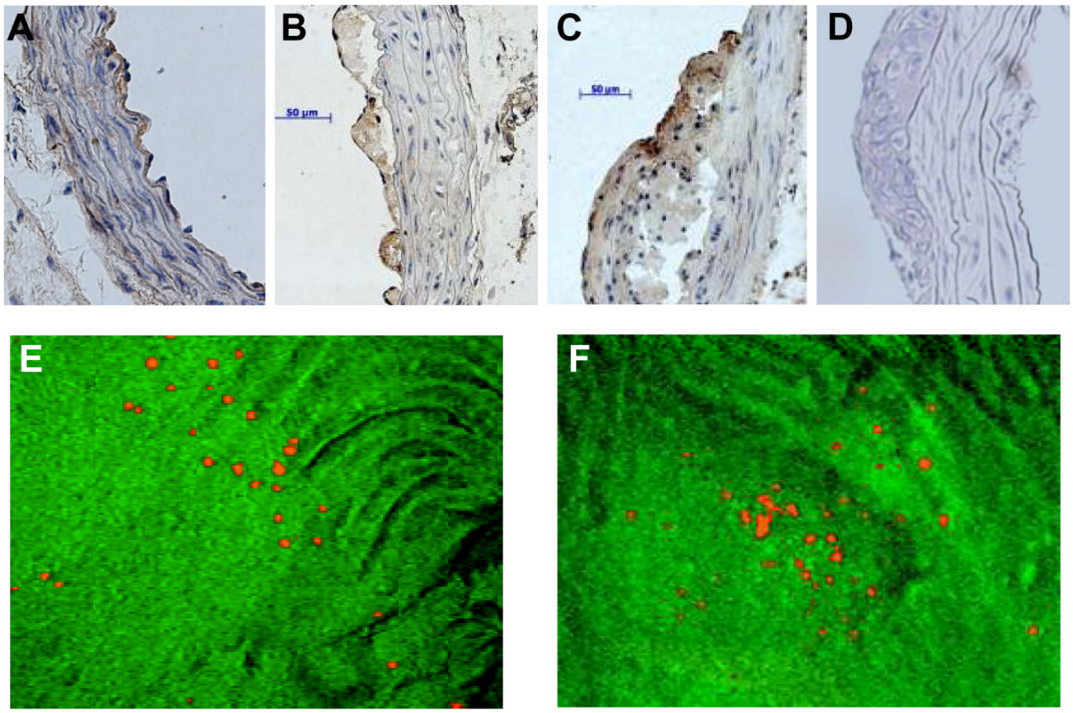

Figure 3.

Immunohistochemistry for VCAM-1 **(A–D)** and whole mount *en face* microscopy **(E,F)** illustrating targeted microbubble adhesion. Examples of VCAM-1 expression in the thoracic aorta of DKO mice are shown at 10, 20, and 40 wks of age (**A–C** respectively), with a negative control (secondary only) (**D**). . En face microscopy images from 20 wk DKO mice illustrate DiI-labeled VCAM-1-targeted (**E**), and P-selectin-targeted (**F**) microbubbles attaching at the margins of an atherosclerotic lesion in the aortic arch. Other examples of microbubble attachment are provided in the on-line supplement. Scale bar=50 μm.

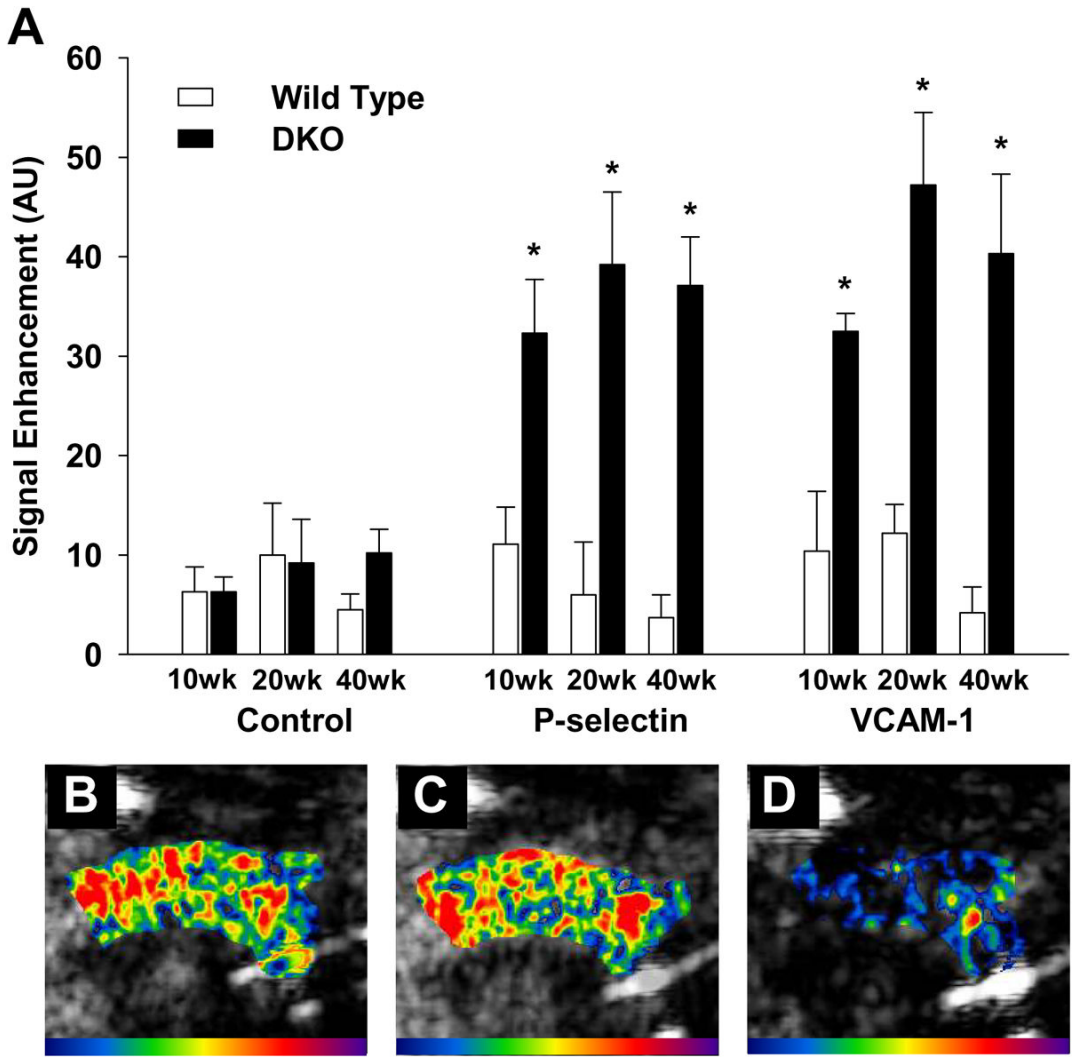

Figure 4.

CEU molecular imaging of the aortic arch. (**A**) Mean (±SEM) background-subtracted signal intensity from control microbubbles and microbubbles targeted to P-selectin and VCAM-1 in the proximal aorta. *$p<0.05$ (adjusted for multiple comparisons) vs control microbubble and compared to corresponding data in wild-type mice; n=10 for all DKO data, n=7 for all 1 wild-type data. Examples of molecular imaging of the aortic arch in a 40 wk DKO animal with (**B**) VCAM-1-targeted, (**C**) P-selectin-targeted, and (**D**) control microbubbles.

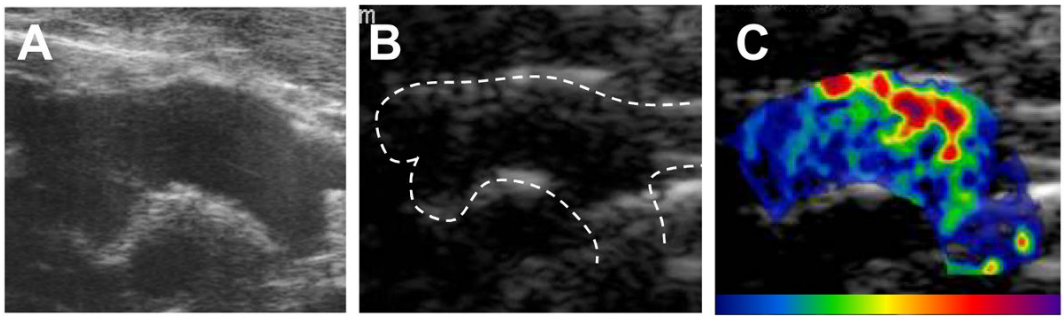

Figure 5.
Illustration of how spatial matching of morphology and targeted signal enhancement. Images from the aortic arch from a 10 wk DKO animal using high-frequency (40 MHz) ultrasound image (**A**), and lower frequency multi-pulse contrast-specific imaging of the aorta at baseline with the aorta defined by dashed lines prior to contrast administration (**B**), and 10 min after administration of P-selectin-targeted microbubbles after background-subtraction and color-coding (color scale at bottom) (**C**).

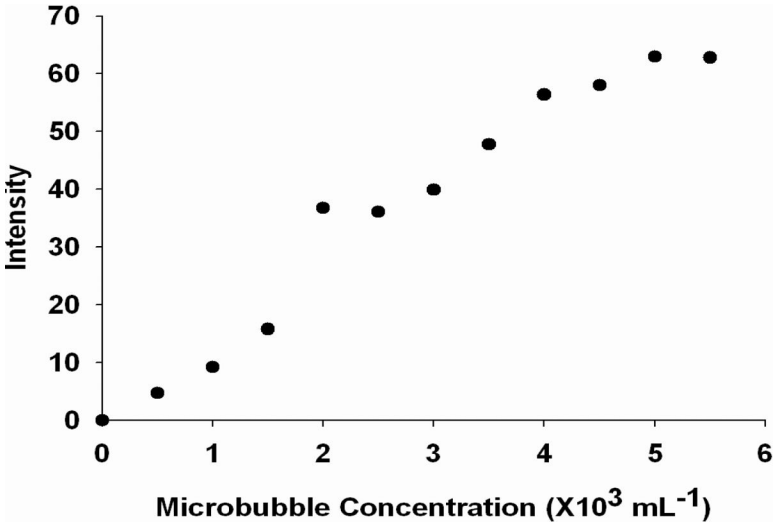

Figure 6.
Microbubble contrast versus video intensity relationship for the CEU imaging parameters used in this study. Data were derived from an *in vitro* circulating water tank system.

Table 1

Echocardiographic Hemodynamic Data (Mean ±SD)

	10 weeks		20 weeks		40 weeks	
	WT (n=11)	**DKO (n=11)**	**WT (n=12)**	**DKO (n=14)**	**WT (n=7)**	**DKO (n=12)**
Fractional Shortening	0.30±0.08	0.32±0.06	0.34±0.07	0.30±0.08	0.32±0.11	0.30±0.09
Aortic internal diameter (mm)	1.32±0.10	1.32±0.14	1.35±0.15	1.34±0.12	1.35±0.15	1.40±0.17
Aortic peak systolic velocity (m/s)	0.73±0.17	0.70±0.14	0.84±0.14	0.76±0.17	0.65±0.12	0.71±0.16

WT, wild-type mice

Arterioscler Thromb Vasc Biol. Author manuscript; available in PMC 2011 January 1.